DR. HASSAN FAHMI (Orcid ID : 0000-0001-7698-557X)
PROF. JEAN-PIERRE PELLETIER (Orcid ID : 0000-0001-9930-6453)
PROF. JOHANNE MARTEL-PELLETIER (Orcid ID : 0000-0003-2618-383X)
DR. MOHAMED BENDERDOUR (Orcid ID : 0000-0002-7853-2133)

Article type : Full Length

Role of Lipocalin-type prostaglandin D synthase in experimental osteoarthritis

Mehdi Najar, PhD[1], Yassine Ouhaddi, MSc[1], Frédéric Paré, MSc[1], Bertrand Lussier, DMV, MSc, Dipl ACVS[2], Yoshihiro Urade, PhD[3], Mohit Kapoor, PhD[4], Jean-Pierre Pelletier, MD[1], Johanne Martel-Pelletier, PhD[1], Mohamed Benderdour, PhD[5] and Hassan Fahmi, PhD[1]

[1]Osteoarthritis Research Unit, University of Montreal Hospital Research Center (CRCHUM), and Department of Medicine, University of Montreal, Montreal, QC, Canada
[2]Faculty of Veterinary Medicine, Clinical Science, University of Montreal, Saint-Hyacinthe, QC, Canada
[3]Isotope Science Center, The University of Tokyo, Yayoi, Bunkyo-ku, Tokyo 113-0032, Japan
[4]The Toronto Western Research Institute, University Health Network (UHN), Toronto, ON, Canada
[5]Research Centre, Sacré-Coeur Hospital, University of Montreal, Montreal, QC, Canada

Correspondence to:
Hassan Fahmi, PhD
Osteoarthritis Research Unit
University of Montreal Hospital Research Center (CRCHUM),
900 Saint-Denis, R11.424, Montreal, QC, Canada H2X 0A9
Tel: + 1 514 890 8000 ext. 25119

Fax: + 1 514 412 7583
E-mail: h.fahmi@umontreal.ca

Running head

L-PGDS in experimental OA

Funding

This work was supported by the Canadian Institutes of Health Research (CIHR) Grant MOP-130293 (to HF and the JSPS KAKENHI grant 16H01881 (to Y.U). Y. Ouhaddi was supported by a fellowship from La Chaire en Arthrose de l'Université de Montréal.

Competing interests

The authors declare no competing interests.

Author's Contributions

M. Najar and Y. Ouhaddi contributed equally to this study.

ABSTRACT

Objective: Lipocalin-type prostaglandin D synthase (L-PGDS) catalyzes the formation of prostaglandin D_2 (PGD_2), which has important roles in inflammation and cartilage metabolism. The aim of this study was to investigate the role of L-PGDS in the pathogenesis of OA using an experimental mouse model.

Methods: Experimental OA was induced in wild-type (WT), and L-PGDS- deficient (L-PGDS-/-) mice (n = 10 per genotype) by destabilization of the medial meniscus (DMM). Cartilage degradation was evaluated by histology. The expression of MMP-13 and ADAMTS-5 was assessed by immunohistochemistry. Bone changes were determined by microcomputed tomography (μ-CT). Cartilage explants from L-PGDS-/- and WT mice (n = 6 per genotype) were treated with interleukin-1α (IL-1α) *ex vivo*, to evaluate proteoglycan

degradation. Moreover, the effect of intra-articular injection of an adeno-associated virus (AAV) 2/5 encoding L-PGDS on OA progression was evaluated in WT mice (n = 9 per group).

Results: Compared to WT mice, L-PGDS-/- mice had exacerbated cartilage degradation, and enhanced expression of MMP-13 and ADAMTS-5 ($P < 0.05$). Furthermore, L-PGDS-/- mice displayed increased synovitis and subchondral bone changes ($P < 0.05$). Cartilage explants from L-PGDS-/- mice showed enhanced proteoglycan degradation following treatment with IL-1α ($P < 0.05$). Intra-articular injection of AAV2/5 encoding L-PGDS attenuated the severity of DMM-induced OA-like changes in WT mice ($P < 0.05$). The level of L-PGDS was *increased* in OA tissues of WT mice ($P < 0.05$).

Conclusion: Collectively, these findings suggest a protective role of L-PGDS in OA, and therefore enhancing it level may constitute a promising therapeutic strategy.

INTRODUCTION

Osteoarthritis (OA) is the most common form of arthritis, and a leading cause of disability. OA is primarily characterized by articular cartilage destruction, synovial inflammation, and subchondral bone remodeling [1, 2]. There is currently, no proven treatment to stop or slow the progression of OA, as the exact mechanisms underlying the initiation, and progression of the disease are yet largely unknown. A deeper understanding of the mechanisms involved in the pathogenesis of OA will be useful in the development of more effective therapeutic agents to prevent or treat OA.

Cartilage breakdown during OA is predominantly mediated by proteases, most notably, matrix metalloproteinase 13 (MMP-13) and a disintegrin and metalloproteinase with thrombospondin motifs 5 (ADAMTS-5). Indeed, MMP-13 overexpressing transgenic mice develop spontaneous OA-like cartilage damage [3], and MMP-13 deletion protected mice against OA-like cartilage damage [4]. In addition, ADAMTS-5 deficiency was shown to prevent cartilage destruction in mouse arthritis models [5, 6].

Increasing evidence indicates that prostaglandin D2 (PGD_2) may have protective effects in OA. We have demonstrated that treatment of chondrocytes with PGD_2 inhibits the induction of MMP-1 and MMP-13, which play an important role in cartilage damage [7]. PGD_2 was also reported to increase the expression of the cartilage-specific matrix molecules type II collagen and aggrecan [8], and to prevent chondrocyte apoptosis [9].

In addition to its chondroprotective effects, PGD_2 has anti-inflammatory properties. For instance, the initiation of inflammation is associated with reduced production of PGD_2, while the resolution phase is associated with increased levels of PGD_2 [10]. Moreover, PGD_2 inhibits several inflammatory responses including the production of IL-12 [11], and interferon γ (IFNγ) [12], and the expression of inducible nitric oxide synthase (iNOS) [13]. PGD_2 was also reported to enhance the production of the anti-inflammatory cytokine IL-10 [14]. The anti-inflammatory effect of PGD_2 is further supported by studies using PGD_2 synthase deficient, and transgenic mice. The knockout animals showed impaired resolution of inflammation, and transgenic animals had little detectable inflammation [15-17].

The biosynthesis of PGD_2 is catalyzed by two PGD synthases (PGDSs) that differ in tissue distribution; the lipocalin-type PGDS (L-PGDS), and the hematopoietic PGDS (H-PGDS) [18]. L-PGDS is expressed abundantly in the central nervous system [19], the heart [20], and skin [21]. H-PGDS is expressed mainly in mast cells [22], megakaryocytes [23] and, T helper (Th) 2 lymphocytes [24].

We have previously shown that articular cartilage predominantly expresses L-PGDS [25, 26]. However, the *in vivo* role of L-PGDS in the pathophysiology of OA remains largely unknown. In this study, we investigated the effect of L-PGDS deficiency on the development of OA using a surgical mouse model, induced by destabilization of the medial meniscus (DMM) [27]. We also evaluated the effect of intra-articular injection of an adeno-associated viral vector (AAV2/5) encoding murine L-PGDS gene on the progression of OA in L-PGDS-/- mice.

MATERIALS AND METHODS

Mice. All animal experiments were approved by the Institutional Animal Protection Committee of the University of Montreal Hospital Research Centre (CRCHUM). L-PGDS-/- mice were generated as described previously [28]. In these mice, L-PGDS gene was disrupted by replacing a 1.84-kb fragment containing parts of exons II-V with the neomycin resistance gene. L-PGDS-/- mice were backcrossed onto the C57BL/6 background for 10 generations. L-PGDS-/- and WT mice used in these experiments were generated by breeding heterozygous littermates, and genotypes were identified by polymerase chain reaction (PCR) of tail biopsy DNA extract. Mice were maintained under standard pathogen-free conditions and 12-hour light/dark cycle, and were freely allowed access to food, water and activity before and after surgery. The mice appeared healthy, and showed normal behavior throughout the study.

Induction of OA in mice. OA was induced by destabilization of the medial meniscus (DMM) in the knee joints of 10-week-old male WT and L-PGDS-/- mice, as previously described [27]. Briefly, animals were anesthetized, and the right knee joint was destabilized by transection of the anterior attachment of the medial meniscotibial ligament (MMTL). The sham operation involved the same surgery, except that the MMTL was visualized but not transected. Buprenorphine was provided perioperatively at 0.09 mg/kg every 10–12 hours for 72 hours. Mice were sacrificed, the knees were harvested, and subjected to micro-CT, histological and immunohistochemical analyses. Only male mice were used *in vivo* in this study because male mice develop better features of the disease [29]. None of the mice died during the experimental period.

Histological evaluation of osteoarthritic changes. Sham- (n = 6) and DMM-operated (n = 10) mice were euthanized at 2, 4 and 8 weeks pots-surgery and the harvested knee joints were fixed in TissuFix (Chaptec, Montreal, QC, Canada), decalcified in 10% EDTA for 14 days at 4°C, and embedded in paraffin. Coronal sections (5-μm) were obtained through the entire joint at 80 μm intervals, and stained with Safranin O–fast green (8 sections per joint) or hematoxylin and eosin (5 sections per joint). Cartilage damage was assessed in accordance with the recommendations of the Osteoarthritis Research Society International (OARSI) guidelines [30]. Synovitis was evaluated using the scoring method described by Lewis et al [31]. All sections were graded by two scorers (MN and YO) in a blinded manner. Scores for cartilage damage, and synovitis

were recorded for the femoral-medial and the tibial-medial condyles on the operated side of the joint, and the scores for the two quadrants regions were summed.

Immunohistochemistry. Immunohistochemical analysis was performed at 2 weeks post-surgery (n = 6 per group) as previously described [32, 33]. We selected this time-point because it is suitable to detect and quantify MMP-13 and ADAMTS-5 in the cartilage of DMM operated mice [32, 33]. For further details, see Supplementary Methods.

Isolation of primary chondrocytes and measurement of PGD_2 levels. Primary epiphyseal chondrocytes were isolated from 5- to 6-day-old mice as previously reported [32]. A detailed description of isolation of primary chondrocytes can be found in the Supplementary Methods.

RNA extraction and real-time reverse transcription-polymerase chain reaction. Total RNA was isolated from whole joints following the removal of the skin and muscle bulk. The joint tissues were homogenized in 1 ml of TRIzol® reagent (Invitrogen, Burlington, ON, Canada) using a PowerGen 125 Polytron instrument (Fisher Scientific), and RNA was isolated, according to the manufacturer's instructions. RNA was reverse transcribed, and amplified using the QuantiTect Reverse Transcription PCR Kit (QIAGEN) on the Rotor Gene 3000 Realtime PCR system (Corbett Research, Mortlake, Australia), according to the manufacturer's protocol. Relative mRNA expression was determined using the $\Delta\Delta C_T$ method, and glyceraldehyde 3-phosphate dehydrogenase (GAPDH) as the housekeeping gene. The primer efficiencies were similar for the target and GAPDH genes. All primer sequences are available on request. Each PCR was performed in triplicate from two independent experiments.

PGD_2 assay. The levels of PGD_2 in culture supernatants or in knee joints were determined using the Prostaglandin D2 ELISA kit (Cayman Chemical, MI, USA). For mouse knee joints, skin and muscle were removed from the operated knee and the samples were snap frozen in liquid N2, and stored at -80°C until use. The samples were then gently homogenized (PowerGen 125 Polytron instrument, Fisher Scientific) in 1 ml ice-cold buffer (10 mM HEPES, pH 7.4, 1 mM EDTA, 1 mM EGTA, 10 mM KCl, 1mM dithiothreitol, 1 mM Na3VO4, 1 mM NaF, 1 mM PMSF, 10 μg/mL each of aprotinin, leupeptin, and pepstatin, and 10 μM, indomethacin). The homogenates were sonicated on ice and centrifuged at 12,000×g for 15 minutes. The

levels of PGD_2 in the supernatants were determined using an enzyme-linked immunosorbent assay (ELISA) kit (Cayman Chemical). All samples were analysed in duplicate and at two different dilutions.

Culture of cartilage explants. Femoral heads from 3- to 4-week-old WT and L-PGDS-/- mice were cultured as explants (4 femoral heads per well) in 48-well plates at 37°C in 400 µl of DMEM containing antibiotics and 10% fetal calf serum for 48 hours. The explants were then washed in serum-free DMEM, and cultured for an additional 72 hours in serum-free DMEM, with and without 10 ng/ml mouse interleukin-1α (IL-1α) (Sigma-Aldrich). Conditioned medium was collected at the end of the culture period and proteoglycan degradation was assessed by measuring the levels of sulfated glycosaminoglycan (GAG) released into culture media using dimethyl methylene blue (DMMB) with chondroitin sulfate as a standard [32]. Results are expressed as µg of GAG released/mg cartilage.

Micro-CT analysis of bone. The knee joints were scanned using the Skyscan 1176 micro-CT scanner (Skyscan, Aartselaar, Belgium) at 50 kV, 500 µA, with a pixel size of 9 µm and a 0.5-mm aluminum filter. Data were recorded at every 3-degree rotation step through 180 degrees. Image slices were reconstructed using NRecon software (version 1.6.3.2, Skyscan). The region of interest (ROI) included the area between the epiphyseal growth plate and articular cartilage. The following morphometric parameters: trabecular bone volume fraction (BV/TV), trabecular thickness (Tb.Th.), trabecular separation (Tb.Sp.), trabecular number (Tb.N.), were determined using CT Analyzer software (SkyScan). CTVox software (SkyScan) was used to create 3-D images.

Intra-articular injection of AAV2/5. Recombinant AAV2/5 vectors encoding either green fluorescent protein GFP alone (AAV2/5-GFP) or L-PGDS-GFP (AAV2/5-L-PGDS-GFP) were generated by Vector BioLabs (Philadelphia, PA, USA). Ten week-old mice were anesthetized, and each right knee was intra-articularly injected with 10 µl of either 1.3×10^{10} gc AAV-GFP or AAV-L-PGDS-GFP. After three days, mice were randomly subjected to sham (n = 6) or DMM (n = 9) surgery. Mice were sacrificed 4 and 8 weeks post-surgery, and the joints were harvested, and processed for immunofluorescence and molecular analyses.

Statistical analysis. Sample size calculations were based on our primary outcome "OA histopathology" and our previous studies [32, 33]. Our sample size would provide >80% power to detect a 50% change in mean OARSI scores with a significance level of $P = 0.05$.

Histological and immunohistochemical data were assessed using the Mann-Whitney U test (for comparison of two groups), or Kruskal-Wallis followed by Dunn's multiple comparisons test (for comparison between more than two groups). Results of the real-time PCR, PGD_2 levels and bone parameters were analyzed using Student's t-test (for comparison of two groups) or one-way ANOVA followed by Bonferroni's multiple comparisons test (for comparison between more than two groups). P-value < 0.05 was considered significant. All analyses were performed using Prism 8.0 (GraphPad).

RESULTS

L-PGDS deficiency enhanced cartilage destruction following DMM surgery. To validate the deletion of L-PGDS, we assessed the expression of L-PGDS mRNA in the knee joints of WT and L-PGDS -/- mice. As expected, the expression of L-PGDS mRNA was absent in L-PGDS-/- mice (Suppl. Fig. 1A). In addition, we compared the expression of L-PGDS protein, and the production of PGD_2, in response to IL-1α in cultured chondrocytes from WT and L-PGDS -/- mice. The results revealed complete absence of L-PGDS expression and PGD_2 production in chondrocytes isolated from L-PGDS-/- mice (Suppl. Fig. 1B, C). These results indicated effective ablation of L-PGDS in L-PGDS-/- mice.

To evaluate the functional role of L-PGDS in OA *in vivo* we studied the development of DMM-induced OA-related changes in L-PGDS -/- mice and their WT littermates. DMM surgery was performed, and knee joints were harvested 2, 4, and 8 weeks post-surgery. Histological analyses revealed that cartilage degradation was more severe and more accelerated in L-PGDS-/- mice compared with WT mice (Fig. 1A). Quantification by the OARSI grading scoring system [30] confirmed the exacerbation and acceleration of cartilage degradation in L-PGDS-/- mice (Fig. 1B). These results indicated that L-PGDS deletion exacerbates OA development in a surgical mouse OA model.

We also examined synovial inflammation, another feature of OA, and found no difference between L-PGDS-/- mice and their WT littermates at 2 and 4 weeks after DMM surgery (Fig. 1C). However, synovitis was greater in L-PGDS -/- mice compared with WT mice, at 8 weeks post-DMM surgery (Fig. 1C). Semi-quantitative scoring [31] confirmed that the scores were higher in L-PGDS-/- mice (Fig. 1D), although this was not statistically significant. These findings demonstrated that L-PGDS deletion accelerates both cartilage destruction, and synovial inflammation.

Increased expression of cartilage-degrading enzymes and cartilage degradation products in L-PGDS-/- mice. To elucidate the mechanisms underlying the exacerbation cartilage degradation in L-PGDS-/- mice, we evaluated the expression of key factors in OA development including ADAMTS-5 and MMP-13. Immunohistochemical analysis revealed that the levels of MMP-13 and ADAMTS-5 enzymes were elevated in the joints of both WT and L-PGDS-/- mice at 2 weeks post-surgery compared to sham-operated control

joints (Fig. 2). This increase was significantly greater in L-PGDS-/- mice than in WT control mice. These results indicate that L-PGDS deletion may enhance cartilage damage by increasing the expression of cartilage degrading enzymes. We also performed immunostaining for type II collagen and aggrecan cleavage fragments. We observed increased staining for C1,2C, VDIPEN, and NITEGE in cartilage from either genotype, though the staining was more intense in the L-PGDS-/- mice, compared to wild-type mice (Suppl. Fig. 2). The elevated staining for the degradation products of MMP-13 and ADAMTS-5 in L-PGDS-/- mice compared with WT mice suggests increased activity of MMP-13 and ADAMTS-5.

L-PGDS deficiency enhanced IL-1α-induced proteoglycan degradation. To further define the role of L-PGDS in cartilage degradation, we examined the effect of IL-1α on proteoglycan degradation in cultured cartilage explants. Femoral head articular cartilage from WT and L-PGDS-/- mice were treated or not with IL-1α, and glycosaminoglycan (GAG) release was evaluated using dimethylmethylene blue assay. Treatment with IL-1α caused a significant increase in GAG release in both WT and L-PGDS-/- cartilage, with the increase being more pronounced in L-PGDS-/- cartilage (Fig. 3). In the absence of IL-1α, there was no significant difference in GAG release between L-PGDS-/- mouse cartilage and WT mouse cartilage. These results further support that L-PGDS deletion increases cartilage degradation.

L-PGDS deletion exacerbated subchondral bone microarchitectural changes following DMM surgery. In addition to articular cartilage destruction, subchondral bone changes are believed to play a key role in the pathogenesis of OA. We therefore used micro-CT to evaluate DMM-induced changes in the microarchitecture of subchondral bone of sham- and DMM-operated WT and L-PGDS-/- mice at 8 weeks post-surgery. As shown in Fig. 4A, both WT and L-PGDS-/- mice had subchondral bone sclerosis, which is more prominent in L-PGDS -/- mice. There was also a significant increase in trabecular bone volume BV/TV in DMM-operated knee compared to sham-operated knees control, in both the WT and L-PGDS-/- mice. Tb.Th also increased in DMM-operated knee joints of WT and L-PGDS-/- mice (Fig. 4B). In line with these changes, there was a decrease in Tb.Sp in DMM-operated knee joints of both genotypes Fig. 4B). The magnitude of subchondral bone changes was more pronounced in L-PGDS-/- mice (Fig. 4B). The 3-D rendering revealed that OA-related bony changes including meniscal calcification, sesamoid bone enlargement, periarticular mineralization, and reduced joint space, which were more prominent in L-PGDS-/- mice (Fig. 4C). These

results demonstrated that L-PGDS deletion, not only exacerbated cartilage degeneration, and synovitis, but also increased the severity of subchondral changes in experimental OA.

Intra-articular injection of AAV2/5-L-PGDS attenuated the severity of experimental osteoarthritis

As L-PGDS deletion was found to exacerbate experimental OA, we investigated whether intra-articular injection of an adeno-associated viral vector (AAV2/5) encoding L-PGDS gene attenuates typical DMM-induced OA-like changes in WT mice. Immunohistochemical analysis at 4 weeks post-DMM surgery revealed that AAV-GFP control virus efficiently transduced cells in the cartilage, meniscus and synovium (Fig. 5A). Efficient AAV infection was further confirmed by detection of high levels of L-PGDS in the above tissues (Fig. 5B). The level of PGD2 was increased in L-PGDS overexpressing joints, demonstrating successful increased activity of L-PGDS (Fig. 5C). As shown in Fig. 5D, the administration of AAV-L-PGDS protected against cartilage loss, and significantly reduced the OARSI scores (Fig. 5E). Synovitis and subchondral bone sclerosis in L-PGDS-injected mice were also lower than in GFP-injected mice (Suppl. Fig. 3). These data suggest that L-PGDS overexpression has protective effects in OA

We also examined whether L-PGDS overexpression reversed the severity of DMM-induced OA-like changes in L-PGDS-/- mice. Efficient gene delivery was confirmed by detection of GFP in cartilage, meniscus and synovium (Suppl. Fig. 4A). Furthermore, high levels of L-PGDS were detected in AAV-L-PGDS-injected mice, while there was no evidence of L-PGDS expression in AAV-GFP-injected joints, as expected (Suppl. Fig. 4B). Mice injected with AAV-L-PGDS, but not those injected with AAV-GFP control, showed diminished cartilage loss and lower histologic scores (Suppl. Fig. 4C). Additionally, subchondral bone sclerosis and synovitis score in L-PGDS-injected mice were lower than in GFP-injected mice (Suppl. Fig. 5). Together, these data further support the notion that L-PGDS has protective effects in OA.

Increased expression of L-PGDS in OA cartilage of WT mice. To further characterize the role of L-PGDS in the pathogenesis of OA, we evaluated the expression level of L-PGDS in knee joints of sham- and DMM-operated WT mice at 2 weeks post-DMM surgery. We observed increased levels of L-PGDS mRNA in the joints of DMM-operated mice compared to those of sham-operated animals (Fig. 6A). The levels of L-PGDS protein was also higher in cartilage from DMM-operated mice than in cartilage from sham-operated mice (Fig. 6B and C). Control sections showed no staining (data not shown). Consistently, the level of PGD_2 was

increased in the knee joints of DMM-operated mice relative to sham-operated mice (Fig. 6D). These findings suggested that the up-regulation of L-PGDS is not sufficient to optimally protect against cartilage damage in this model.

DISCUSSION

In the present study, we demonstrated for the first time, that L-PGDS deletion accelerates and aggravates DMM-induced OA progression. Compared to their WT littermates, L-PGDS-/- mice displayed enhanced cartilage degradation, synovial inflammation, and subchondral bone alterations. These changes were associated with increased expression of cartilage matrix-degrading enzymes MMP-13 and ADAMTS-5 and their ECM degradation products. Finally, we found that enforced intra-articular overexpression of L-PGDS reversed the severity of cartilage degradation in L-PGDS-/- mice. These findings suggest a protective role of L-PGDS in OA, thus enhancing it expression/activity may constitute a new therapeutic strategy in the treatment of OA.

To define the functional role of L-PGDS in OA, we studied the course of DMM-induced OA in L-PGDS-/- mice and their WT littermates. We found that the extent of cartilage damage seen in L-PGDS-/- mice was significantly increased compared to WT mice. Cartilage degradation in L-PGDS-/- mice was associated with increased expression of MMP-13, and ADAMTS-5, and their degradation products VDIPEN, NITEG and C12C. In addition, *ex vivo* cartilage explant studies revealed a significant increase in IL-1-induced proteoglycan release in cartilage from L-PGDS-/- mice compared to WT mice. Collectively, these data suggest that L-PGDS deletion exacerbates cartilage damage by enhancing MMP-13 and ADAMTS-5 expression. This is also consistent with our previous study showing that PGD_2 and $15d\text{-}PGJ_2$, the main products of L-PGDS, prevent MMP-1 and MMP-13 production in cultured chondrocytes [7, 34].

Another important finding of this study was that L-PGDS-/- mice had increased synovitis compared to WT mice at 8 weeks post-surgery. This is likely related to the anti-inflammatory properties of L-PGDS products, and is in agreement with previous studies in which injection of PGD_2 reduced synovial inflammation, and joint damage in murine collagen-induced arthritis [14]. $15d\text{-}PGJ_2$, another end product of L-PGDS, has also been reported to reduce synovitis in collagen-induced arthritis in mice [35], and adjuvant-induced arthritis in

rats [36]. Further studies have demonstrated that PGD_2 attenuates inflammation in a number of experimental models including atopic dermatitis [37] and colitis [38]. Moreover, L-PGDS deletion was reported to exacerbate atherosclerosis and nephropathy [17, 39].

Subchondral bone changes are another critical feature of OA pathogenesis in OA patients and in animal models of OA. Micro-CT assessment of the subchondral bone in WT and L-PGDS -/- mouse knee joints revealed subchondral bone sclerosis, increased BV/TV and TbTh, and ectopic bone formation at 8 weeks post-surgery. These impairments were, however, more pronounced in L-PGDS-/- mice compared to WT mice. This is likely due to the importance of PGD_2 in bone remodeling [40, 41]. Thus, in addition to cartilage degeneration and synovitis, L-PGDS deficiency also increased the magnitude of subchondral changes. Articular cartilage and the underlying bone operate as a functional unit in the joint, and crosstalk between both tissues compartments is believed to play an important role in the onset and progression of OA. Given that the mice used in our study are global constitutive KO and that L-PGDS is expressed in cartilage, bone and synovium, we cannot determine whether the observed effects were due to L-PGDS loss in cartilage, bone or synovium. Future detailed analyses of L-PGDS deletion in specific tissues will contribute to a better understanding of the role of L-PGDS in the progression of OA.

Having demonstrated that L-PGDS deletion exacerbated OA-like changes, we assessed the effect of L-PGDS overexpression in the joint on the course of OA in WT mice. We found that intra-articular administration of an AAV2/5 encoding L-PGDS attenuates the severity of cartilage degradation, synovitis and subchondral bone sclerosis, confirming the protective role of L-PGDS. We also found that intra-articular injection of AAV2/5-LPGDS reversed the exacerbation of DMM-induced cartilage degradation in L-PGDS-/- mice. Interestingly, the protective effect of L-PGDS overexpression was associated with increased level of PGD_2, suggesting that enhanced production of PGD_2 is the likely mechanism by which L-PGDS overexpression attenuates cartilage degradation. This is in accordance with our previous findings showing that treatment with BW245C, an agonist of the PGD_2 receptor DP1, protects against OA and that DP1 deletion exacerbates murine experimental OA [32].

Finally, we showed that L-PGDS expression is elevated in the cartilage of DMM-operated WT. This is consistent with our previous studies showing enhanced levels of L-PGDS in human [25], guinea pig and dog [26] OA cartilage. These findings suggested that although protective, up-regulation of endogenous L-PGDS might not be high enough to prevent the development of OA in this model.

It is also well known that the dehydration product of PGD_2, 15d-PGJ_2, exerts anti-inflammatory effects through either PPAR-γ–dependent or PPAR-γ–independent pathways. We have previously shown that 15d-PGJ_2 or PPAR-γ agonists negatively regulate the expression of a number of inflammatory and catabolic events in culture chondrocytes and synovial fibroblasts [42]. Moreover, we have demonstrated that PPARγ deficiency in mice accelerates experimental OA [43]. Additional studies demonstrated that administration of 15d-PGJ_2 attenuates the severity of collagen-induced arthritis in mice [35], and adjuvant-induced arthritis in rats [36]. Thus, L-PGDS deletion may lead to reduced levels of 15-PGJ_2 in the joint, resulting in enhanced inflammatory and catabolic responses and subsequent acceleration of OA progression.

In addition to its ability to catalyze the production of PGD_2 and 15d-PGJ_2, L-PGDS is also involved in the binding and transport of small lipophilic molecules, known for their implication in the pathophysiology of OA, like retinoids [44], thyroid hormones [21], and gangliosides [45]. Therefore, it is possible that the lack of L-PGDS will exacerbate OA by disrupting the availability and transport of these lipophilic molecules and/or altering their downstream signalling pathways.

This study has some limitations. First, we used only male mice because male mice develop better features of the disease [29]. Second, although we demonstrated that L-PGDS deletion aggravates instability-induced OA, we did not evaluate the effect of L-PGDS deletion on the development of spontaneous OA, which is also relevant to the pathogenesis of OA. Third, we did not investigate the effect of L-PGDS deletion on OA-related pain behavior. Previous studies reported anti-nociceptive effects of PGD_2. For example, Minami et al. showed that treatment with PGD_2 prevents PGE_2 induced allodynia [46], and nociceptin evoked hyperalgesia [47]. The anti-nociceptive effect of PGD_2 is corroborated by the finding of Telleria-Diaz [48], who showed that topical application of PGD_2 to the spinal cord of rats with inflamed knee joints decreased responses to mechanical stimulation. Other studies, however, reported pro-nociceptive effects of PGD_2. For instance, PGE_2-induced

allodynia was attenuated in L-PGDS-/- mice [28], and PGD_2 was reported to induce hyperalgesia and allodynia [49]. Further studies are required to define the exact role of PGD_2 and L-PGDS in OA-related pain.

Inhibition of prostaglandin production by traditional NSAIDs and COX-2 specific inhibitors have been widely used clinically for the management of OA, however, their effects on the structural progression of disease remains controversial. Our findings that L-PGDS has protective properties, suggest that inhibition of endogenous PGD2 biosynthesis may partially explain the lack of long-term disease-modifying activity in patients receiving these drugs and underline the limits of therapeutic approaches that inhibit the production of all prostaglandins.

In conclusion, our findings suggest a protective role of L-PGDS in OA. They also suggest that enhancing the level of L-PGDS could be an attractive new strategy for the treatment of OA.

Acknowledgements

We would also like to thank members (the managers, veterinarians, and animal caretakers) at the CRCHUM animal facility for their assistance, and for maintaining the mice for this study. This work was supported by the Canadian Institutes of Health Research (CIHR) Grant MOP-130293. Y. Ouhaddi was supported by a fellowship from La Chaire en Arthrose de l'Université de Montréal

REFERENCES

1. Loeser RF, Goldring SR, Scanzello CR, Goldring MB: Osteoarthritis: a disease of the joint as an organ. *Arthritis Rheum* 2012, 64(6):1697-1707.
2. Wei Y, Bai L: Recent advances in the understanding of molecular mechanisms of cartilage degeneration, synovitis and subchondral bone changes in osteoarthritis. *Connect Tissue Res* 2016, 57(4):245-261.
3. Neuhold LA, Killar L, Zhao W, Sung ML, Warner L, Kulik J, Turner J, Wu W, Billinghurst C, Meijers T *et al*: Postnatal expression in hyaline cartilage of constitutively active human collagenase-3 (MMP-13) induces osteoarthritis in mice. *J Clin Invest* 2001, 107(1):35-44.
4. Little CB, Barai A, Burkhardt D, Smith SM, Fosang AJ, Werb Z, Shah M, Thompson EW: Matrix metalloproteinase 13-deficient mice are resistant to osteoarthritic cartilage erosion but not chondrocyte hypertrophy or osteophyte development. *Arthritis Rheum* 2009, 60(12):3723-3733.
5. Glasson SS, Askew R, Sheppard B, Carito B, Blanchet T, Ma HL, Flannery CR, Peluso D, Kanki K, Yang Z *et al*: Deletion of active ADAMTS5 prevents cartilage degradation in a murine model of osteoarthritis. *Nature* 2005, 434(7033):644-648.
6. Stanton H, Rogerson FM, East CJ, Golub SB, Lawlor KE, Meeker CT, Little CB, Last K, Farmer PJ, Campbell IK *et al*: ADAMTS5 is the major aggrecanase in mouse cartilage in vivo and in vitro. *Nature* 2005, 434(7033):648-652.
7. Zayed N, Afif H, Chabane N, Mfuna-Endam L, Benderdour M, Martel-Pelletier J, Pelletier JP, Motiani RK, Trebak M, Duval N *et al*: Inhibition of interleukin-1beta-induced matrix metalloproteinases 1 and 13 production in human osteoarthritic chondrocytes by prostaglandin D(2). *Arthritis Rheum* 2008, 58(11):3530-3540.

8. Jakob M, Demarteau O, Suetterlin R, Heberer M, Martin I: Chondrogenesis of expanded adult human articular chondrocytes is enhanced by specific prostaglandins. *Rheumatology (Oxford)* 2004, 43(7):852-857.
9. Relic B, Benoit V, Franchimont N, Ribbens C, Kaiser MJ, Gillet P, Merville MP, Bours V, Malaise MG: 15-deoxy-delta12,14-prostaglandin J2 inhibits Bay 11-7085-induced sustained extracellular signal-regulated kinase phosphorylation and apoptosis in human articular chondrocytes and synovial fibroblasts. *J Biol Chem* 2004, 279(21):22399-22403.
10. Gilroy DW, Colville-Nash PR, Willis D, Chivers J, Paul-Clark MJ, Willoughby DA: Inducible cyclooxygenase may have anti-inflammatory properties. *Nat Med* 1999, 5(6):698-701.
11. Theiner G, Gessner A, Lutz MB: The mast cell mediator PGD2 suppresses IL-12 release by dendritic cells leading to Th2 polarized immune responses in vivo. *Immunobiology* 2006, 211(6-8):463-472.
12. Torres D, Paget C, Fontaine J, Mallevaey T, Matsuoka T, Maruyama T, Narumiya S, Capron M, Gosset P, Faveeuw C *et al*: Prostaglandin D2 inhibits the production of IFN-gamma by invariant NK T cells: consequences in the control of B16 melanoma. *J Immunol* 2008, 180(2):783-792.
13. Nagoshi H, Uehara Y, Kanai F, Maeda S, Ogura T, Goto A, Toyo-oka T, Esumi H, Shimizu T, Omata M: Prostaglandin D2 inhibits inducible nitric oxide synthase expression in rat vascular smooth muscle cells. *Circ Res* 1998, 82(2):204-209.
14. Maicas N, Ibanez L, Alcaraz MJ, Ubeda A, Ferrandiz ML: Prostaglandin D2 regulates joint inflammation and destruction in murine collagen-induced arthritis. *Arthritis Rheum* 2012, 64(1):130-140.
15. Trivedi SG, Newson J, Rajakariar R, Jacques TS, Hannon R, Kanaoka Y, Eguchi N, Colville-Nash P, Gilroy DW: Essential role for hematopoietic prostaglandin D2 synthase in the control of delayed type hypersensitivity. *Proc Natl Acad Sci U S A* 2006, 103(13):5179-5184.
16. Murata T, Aritake K, Tsubosaka Y, Maruyama T, Nakagawa T, Hori M, Hirai H, Nakamura M, Narumiya S, Urade Y *et al*: Anti-inflammatory role of PGD2 in acute lung inflammation and therapeutic application of its signal enhancement. *Proc Natl Acad Sci U S A* 2013, 110(13):5205-5210.

17. Tanaka R, Miwa Y, Mou K, Tomikawa M, Eguchi N, Urade Y, Takahashi-Yanaga F, Morimoto S, Wake N, Sasaguri T: Knockout of the l-pgds gene aggravates obesity and atherosclerosis in mice. *Biochem Biophys Res Commun* 2009, 378(4):851-856.
18. Urade Y, Eguchi N: Lipocalin-type and hematopoietic prostaglandin D synthases as a novel example of functional convergence. *Prostaglandins Other Lipid Mediat* 2002, 68-69:375-382.
19. Urade Y, Fujimoto N, Hayaishi O: Purification and characterization of rat brain prostaglandin D synthetase. *J Biol Chem* 1985, 260(23):12410-12415.
20. Eguchi Y, Eguchi N, Oda H, Seiki K, Kijima Y, Matsu-ura Y, Urade Y, Hayaishi O: Expression of lipocalin-type prostaglandin D synthase (beta-trace) in human heart and its accumulation in the coronary circulation of angina patients. *Proc Natl Acad Sci U S A* 1997, 94(26):14689-14694.
21. Beuckmann CT, Gordon WC, Kanaoka Y, Eguchi N, Marcheselli VL, Gerashchenko DY, Urade Y, Hayaishi O, Bazan NG: Lipocalin-type prostaglandin D synthase (beta-trace) is located in pigment epithelial cells of rat retina and accumulates within interphotoreceptor matrix. *J Neurosci* 1996, 16(19):6119-6124.
22. Urade Y, Ujihara M, Horiguchi Y, Igarashi M, Nagata A, Ikai K, Hayaishi O: Mast cells contain spleen-type prostaglandin D synthetase. *J Biol Chem* 1990, 265(1):371-375.
23. Fujimori K, Kanaoka Y, Sakaguchi Y, Urade Y: Transcriptional activation of the human hematopoietic prostaglandin D synthase gene in megakaryoblastic cells. Roles of the oct-1 element in the 5'-flanking region and the AP-2 element in the untranslated exon 1. *J Biol Chem* 2000, 275(51):40511-40516.
24. Tanaka K, Ogawa K, Sugamura K, Nakamura M, Takano S, Nagata K: Cutting edge: differential production of prostaglandin D2 by human helper T cell subsets. *J Immunol* 2000, 164(5):2277-2280.
25. Zayed N, Li X, Chabane N, Benderdour M, Martel-Pelletier J, Pelletier JP, Duval N, Fahmi H: Increased expression of lipocalin-type prostaglandin D2 synthase in osteoarthritic cartilage. *Arthritis Res Ther* 2008, 10(6):R146.
26. Nebbaki SS, El Mansouri FE, Afif H, Kapoor M, Benderdour M, Pelletier JP, Martel-Pelletier J, Fahmi H: Expression of peroxisome proliferator-activated receptors alpha, beta, gamma,

and H- and L-prostaglandin D synthase during osteoarthritis in the spontaneous hartley guinea pig and experimental dog models. *J Rheumatol* 2013, 40(6):877-890.

27. Glasson SS, Blanchet TJ, Morris EA: The surgical destabilization of the medial meniscus (DMM) model of osteoarthritis in the 129/SvEv mouse. *Osteoarthritis Cartilage* 2007, 15(9):1061-1069.
28. Eguchi N, Minami T, Shirafuji N, Kanaoka Y, Tanaka T, Nagata A, Yoshida N, Urade Y, Ito S, Hayaishi O: Lack of tactile pain (allodynia) in lipocalin-type prostaglandin D synthase-deficient mice. *Proc Natl Acad Sci U S A* 1999, 96(2):726-730.
29. Ma HL, Blanchet TJ, Peluso D, Hopkins B, Morris EA, Glasson SS: Osteoarthritis severity is sex dependent in a surgical mouse model. *Osteoarthritis Cartilage* 2007, 15(6):695-700.
30. Glasson SS, Chambers MG, Van Den Berg WB, Little CB: The OARSI histopathology initiative - recommendations for histological assessments of osteoarthritis in the mouse. *Osteoarthritis Cartilage* 2010, 18 Suppl 3:S17-23.
31. Lewis JS, Hembree WC, Furman BD, Tippets L, Cattel D, Huebner JL, Little D, DeFrate LE, Kraus VB, Guilak F *et al*: Acute joint pathology and synovial inflammation is associated with increased intra-articular fracture severity in the mouse knee. *Osteoarthritis Cartilage* 2011, 19(7):864-873.
32. Ouhaddi Y, Nebbaki SS, Habouri L, Afif H, Lussier B, Kapoor M, Narumiya S, Pelletier JP, Martel-Pelletier J, Benderdour M *et al*: Exacerbation of Aging-Associated and Instability-Induced Murine Osteoarthritis With Deletion of D Prostanoid Receptor 1, a Prostaglandin D2 Receptor. *Arthritis Rheumatol* 2017, 69(9):1784-1795.
33. Habouri L, El Mansouri FE, Ouhaddi Y, Lussier B, Pelletier JP, Martel-Pelletier J, Benderdour M, Fahmi H: Deletion of 12/15-lipoxygenase accelerates the development of aging-associated and instability-induced osteoarthritis. *Osteoarthritis Cartilage* 2017, 25(10):1719-1728.
34. Fahmi H, Di Battista JA, Pelletier JP, Mineau F, Ranger P, Martel-Pelletier J: Peroxisome proliferator--activated receptor gamma activators inhibit interleukin-1beta-induced nitric oxide and matrix metalloproteinase 13 production in human chondrocytes. *Arthritis Rheum* 2001, 44(3):595-607.

35. Cuzzocrea S, Wayman NS, Mazzon E, Dugo L, Di Paola R, Serraino I, Britti D, Chatterjee PK, Caputi AP, Thiemermann C: The cyclopentenone prostaglandin 15-deoxy-Delta(12,14)-prostaglandin J(2) attenuates the development of acute and chronic inflammation. *Mol Pharmacol* 2002, 61(5):997-1007.
36. Kawahito Y, Kondo M, Tsubouchi Y, Hashiramoto A, Bishop-Bailey D, Inoue K, Kohno M, Yamada R, Hla T, Sano H: 15-deoxy-delta(12,14)-PGJ(2) induces synoviocyte apoptosis and suppresses adjuvant-induced arthritis in rats. *J Clin Invest* 2000, 106(2):189-197.
37. Angeli V, Staumont D, Charbonnier AS, Hammad H, Gosset P, Pichavant M, Lambrecht BN, Capron M, Dombrowicz D, Trottein F: Activation of the D prostanoid receptor 1 regulates immune and skin allergic responses. *J Immunol* 2004, 172(6):3822-3829.
38. Ajuebor MN, Singh A, Wallace JL: Cyclooxygenase-2-derived prostaglandin D(2) is an early anti-inflammatory signal in experimental colitis. *Am J Physiol Gastrointest Liver Physiol* 2000, 279(1):G238-244.
39. Ragolia L, Palaia T, Hall CE, Maesaka JK, Eguchi N, Urade Y: Accelerated glucose intolerance, nephropathy, and atherosclerosis in prostaglandin D2 synthase knock-out mice. *J Biol Chem* 2005, 280(33):29946-29955.
40. Gallant MA, Samadfam R, Hackett JA, Antoniou J, Parent JL, de Brum-Fernandes AJ: Production of prostaglandin D(2) by human osteoblasts and modulation of osteoprotegerin, RANKL, and cellular migration by DP and CRTH2 receptors. *J Bone Miner Res* 2005, 20(4):672-681.
41. Yue L, Haroun S, Parent JL, de Brum-Fernandes AJ: Prostaglandin D(2) induces apoptosis of human osteoclasts through ERK1/2 and Akt signaling pathways. *Bone* 2014, 60:112-121.
42. Fahmi H, Pelletier JP, Martel-Pelletier J: PPARgamma ligands as modulators of inflammatory and catabolic responses on arthritis. An overview. *J Rheumatol* 2002, 29:3-14.
43. Vasheghani F, Zhang Y, Li YH, Blati M, Fahmi H, Lussier B, Roughley P, Lagares D, Endisha H, Saffar B *et al*: PPARgamma deficiency results in severe, accelerated osteoarthritis associated with aberrant mTOR signalling in the articular cartilage. *Ann Rheum Dis* 2015, 74(3):569-578.

44. Tanaka T, Urade Y, Kimura H, Eguchi N, Nishikawa A, Hayaishi O: Lipocalin-type prostaglandin D synthase (beta-trace) is a newly recognized type of retinoid transporter. *J Biol Chem* 1997, 272(25):15789-15795.
45. Mohri I, Taniike M, Okazaki I, Kagitani-Shimono K, Aritake K, Kanekiyo T, Yagi T, Takikita S, Kim HS, Urade Y *et al*: Lipocalin-type prostaglandin D synthase is up-regulated in oligodendrocytes in lysosomal storage diseases and binds gangliosides. *J Neurochem* 2006, 97(3):641-651.
46. Minami T, Okuda-Ashitaka E, Mori H, Ito S, Hayaishi O: Prostaglandin D2 inhibits prostaglandin E2-induced allodynia in conscious mice. *J Pharmacol Exp Ther* 1996, 278(3):1146-1152.
47. Minami T, Okuda-Ashitaka E, Nishizawa M, Mori H, Ito S: Inhibition of nociceptin-induced allodynia in conscious mice by prostaglandin D2. *Br J Pharmacol* 1997, 122(4):605-610.
48. Telleria-Diaz A, Ebersberger A, Vasquez E, Schache F, Kahlenbach J, Schaible HG: Different effects of spinally applied prostaglandin D2 on responses of dorsal horn neurons with knee input in normal rats and in rats with acute knee inflammation. *Neuroscience* 2008, 156(1):184-192.
49. Minami T, Uda R, Horiguchi S, Ito S, Hyodo M, Hayaishi O: Allodynia evoked by intrathecal administration of prostaglandin E2 to conscious mice. *Pain* 1994, 57(2):217-223.

FIGURE LEGENDS

Figure 1. L-PGDS deletion exacerbated OA following DMM surgery. Ten-week-old WT and L-PGDS-/- mice (n = 10 mice/genotype/time point) were subjected to DMM surgery. Knee joint samples were harvested 2, 4, or 8 weeks post-surgery, prepared and stained with Safranin O–fast green (to assess the extent of articular cartilage degeneration) or hematoxylin and eosin (to asses synovium changes). **(A)** Representative Safranin O staining, and (**B)** summed histologic scores for medial femorotibial joints of WT (open symbols) and L-PGDS-/- (filled symbols) mice at 2, 4, and 8 weeks after DMM surgery. **(C)** Representative hematoxylin and eosin staining, and **(D)** quantification of the synovial inflammation in knee joints. Scale bars = 100 μm. The representative sections were selected based on the average score from each experimental group. Results are presented as median with interquartile range. *P<0.05 versus WT mice.

Figure 2. Expression of ADAMTS-5, and MMP-13 in the knee joints of WT and L-PGDS-/- mice at 2 weeks post-DMM surgery. A) Representative images of immunohistochemical staining for ADAMTS5, and MMP-13in knee joints from sham- (n = 6) and DMM-operated mice (n = 6) at 2 weeks post-surgery. Scale bars = 100 μm. **B)** Percentage of chondrocytes expressing ADAMTS5, and MMP-13 in WT (open symbols) and L-PGDS-/- (filled symbols) mice (n = 6 per genotype). Data are presented as median with interquartile range of each group. *P<0.05 versus WT mice.

Figure 3. L-PGDS deletion enhanced IL-1α–induced proteoglycan degradation in cultured cartilage explants. Femoral heads from 3- to 4-week-old WT and L-PGDS-/- mice were cultured as explants (4 femoral heads (2 mice) per well) in 48-well plates and were stimulated with 10 ng/ml IL-1α for 72 h. Proteoglycan degradation in conditioned media from cultured explants was evaluated using dimethyl methylene blue assay). Data are expressed as mean ± SD of three independent experiments. *P<0.05 versus WT mice.

Figure 4. Micro-CT analysis of the subchondral bone of the tibial plateau of WT and L-PGDS-/- mice at 8 weeks post-DMM surgery. Knee joints from sham- (n = 6 mice per genotype) and DMM-operated (n = 10 mice per genotype) WT and L-PGDS-/- mice were evaluated by micro-CT at 8 weeks post-surgery. **A)** Representative axial micro-CT images of the subchondral bone compartment. Scale bars = 1 mm **B)** Quantification of BV/TV, Tb.Th, and Tb.Sp in the subchondral bone region of the medial tibial plateau of WT

(open symbols) and L-PGDS-/- (filled symbols) mice. Data are presented as mean mean ± SD. *P<0.05 versus WT mice. **C**) Representative 3D reconstructions of the knee joints of sham- and DMM-operated WT and L-PGDS-/- mice. Scale bars = 1 mm.

Figure 5. AAV2/5-mediated L-PGDS over-expression in the joint attenuated DMM-induced cartilage degradation. Ten-week-old WT mice were intra-articularly injected with AAV2/5-GFP or AAV2/5-L-PGDS-GFP. Three days later, mice were subjected to sham or DMM surgery. Mice were euthanized at 4 weeks after surgery for immunohistochemical analysis and PGD2 quantification, and at 8 weeks post-surgery for histological analysis. **A)** Representative images of GFP fluorescence in knee joints from mice injected with AAV2/5-GFP (n = 6). Nuclei were detected by DAPI (4',6-diamidino-2-phenylindole) staining (right). **B)** Representative images of immunohistochemical staining for L-PGDS in knee joints from mice injected with AAV2/5-GFP or AAV2/5-L-PGDS-GFP (n = 6). **C)** PGD2 levels in knee joint of sham- (n = 6) and DMM-operated (n = 9) mice were determined by ELISA. **D)** Representative Safranin O-fast green stained histological sections and **(E)** respective OARSI score for medial femorotibial joints of sham- (n = 6) and DMM-operated (n = 9) mice. Scale bars = 100 μm. Results are presented as median with interquartile range. *P<0.05 versus mice injected with AAV2/5-GFP control.

Figure 6. Increased expression of L-PGDS in mouse OA cartilage. A) Total RNA was extracted from the joints of sham- (n = 6) and DMM-operated (n = 6) WT mice at 2 weeks post-surgery, and the levels of L-PGDS mRNA were determined by real-time RT-PCR. Results are expressed as -fold change, considering the value for sham-operated mice as 1. **B)** Representative images of immunohistochemical staining for L-PGDS in knee joints from sham- (n = 6) and DMM-operated mice (n = 6) at 2 weeks post-surgery. Scale bars = 100 μm. **C)** Percentage of chondrocytes expressing L-PGDS in sham- and DMM-operated cartilage**. D)** PGD2 levels in knee joint of sham-(n = 6) and DMM-operated WT (n = 6) mice at 2 weeks post-surgery, as determined by ELISA. Results are shown as median with interquartile range. *P<0.05 versus sham-operated mice.

Supplemental Figure 1. Effective deletion of L-PGDS in L-PGDS-/- chondrocytes. A) Total RNA was extracted from the joints of L-PGDS-/- and WT mice (n = 4 per genotype), and processed for RT-PCR analysis using L-PGDS and GAPDH-specific primers. PCR products were resolved on a 2% agarose gel. **B)**

Chondrocytes from WT or L-PGDS-/- mice were treated with 100 pg/mL IL-1α for the indicated time periods. Cell lysates were prepared and analyzed for L-PGDS and β-actin proteins by Western blotting. The blots are representative of results from three independent experiments. **C)** Conditioned media were collected and analyzed for PGD2 content by ELISA. Results are expressed as the mean ± SD of 3 independent experiments. **P* < 0.05 compared with unstimulated cells.

Supplementary Figure 2. Expression of C1, 2C, NITEG and VDIPEN in the knee joints of WT and L-PGDS-/- mice at 2 weeks post-DMM surgery. Knee joint sections from sham- (n = 6 per genotype) and DMM-operated (n = 6 per genotype) mice at 2 post-surgery were analyzed by immunohistochemistry for C1,2C, NITEG and VDIPEN. Scale bars = 100 μm. **B)** Percentage of positive stained area (C1,2C and VDIPEN), and positive chondrocytes (NITEG) in WT (open symbols) and L-PGDS-/- (filled symbols) mice. Data are presented as median with interquartile range. *P<0.05 versus WT mice.

Supplementary Figure 3. AAV2/5-mediated L-PGDS over-expression in the joint attenuated the severity of DMM-induced synovitis and subchondral bone changes in WT mice. Ten-week-old WT mice were intra-articularly injected with AAV2/5-GFP or AAV2/5-L-PGDS-GFP. Three days later, mice were subjected to sham (n = 6) or DMM (n = 9) surgery. Mice were euthanized at 4 weeks post-surgery for hematoxylin and eosin staining, and at 8 weeks post-surgery for microCT analysis. **A**). Representative hematoxylin and eosin staining and **(B)** respective synovitis scores. Scale bars = 100 μm. Data are presented as median with interquartile range. *P<0.05 versus mice injected with AAV2/5-GFP control. **C)** Representative axial micro-CT images of the subchondral bone compartment of sham- and DMM-operated WT mice 8 weeks after surgery. Scale bars = 1 mm. **D)** Quantification of BV/TV, Tb.Th, and Tb.Sp in the subchondral bone region of the medial tibial plateau of sham- and DMM-operated mice 8 weeks after surgery. Horizontal lines on the graph represent the mean of each group. *P<0.05 versus mice injected with AAV2/5-GFP control. **E**) Representative 3D reconstructions of the knee joints of sham- and DMM-operated mice 8 weeks after surgery. Scale bars = 1 mm.

Supplementary Figure 4. AAV2/5-mediated L-PGDS overexpression in the joint attenuated DMM-induced OA progression in L-PGDS -/- mice. Ten-week-old L-PGDS-/- mice were intra-articularly injected

with AAV2/5-GFP or AAV2/5-L-PGDS-GFP. Three days later, mice were subjected to sham (n = 6) or DMM (n = 9) surgery. Mice were sacrificed 4 weeks after DMM surgery, and the joints were processed for immunohistochemistry and histology. **A)** GFP expression was determined by fluorescence microscopy. Nuclei were detected by DAPI (4',6-diamidino-2-phenylindole) staining (left). **B)** L-PGDS expression was determined by immunostaining. **C)** PGD2 levels in knee joint of sham- (n = 6) and DMM-operated (n = 9) mice at 4 weeks post-surgery, as tested by ELISA. **D)** Representative Safranin O-fast green stained histological sections and **(E)** respective OARSI score for medial femorotibial joints. Scale bars = 100 μm. Results are presented as median with interquartile range. *P<0.05 versus mice injected with AAV2/5-GFP control.

Supplementary Figure 5. AAV2/5-mediated L-PGDS expression in the joint attenuated the severity of DMM-induced synovitis and subchondral bone changes in L-PGDS -/- mice. Ten-week-old L-PGDS-/- mice were intra-articularly injected with AAV2/5-GFP or AAV2/5-L-PGDS-GFP. Three days later, mice were subjected to sham (n = 6) or DMM (n = 9) surgery. Mice were sacrificed 4 weeks after DMM surgery, and the joints were evaluated by microCT and stained with hematoxylin and eosin. **A)** Representative hematoxylin and eosin staining and **(B)** respective synovitis scores. Scale bars = 100 μm. Data are presented as median with interquartile range. *P<0.05 versus mice injected with AAV2/5-GFP control. **C)** Representative axial micro-CT images of the subchondral bone compartment of sham- and DMM-operated L-PGDS-/- mice 8 weeks after surgery. Scale bars = 1 mm. **D)** Quantification of BV/TV, Tb.Th, and Tb.Sp in the subchondral bone region of the medial tibial plateau of sham- and DMM-operated mice 8 weeks after surgery. Horizontal lines on the graph represent the mean of each group. *P<0.05 versus mice injected with AAV2/5-GFP control. **E**) Representative 3D reconstructions of the knee joints of sham- and DMM-operated mice 8 weeks after surgery. Scale bars = 1 mm.

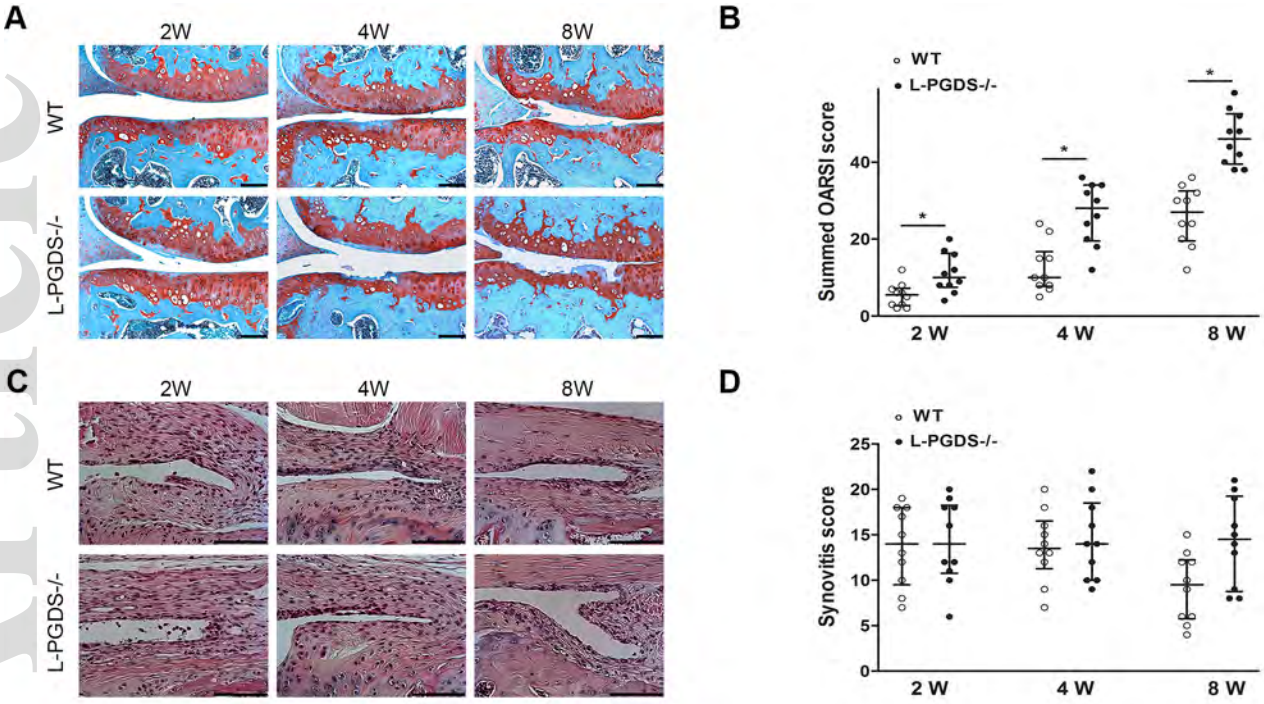

art_41297_f1.tif

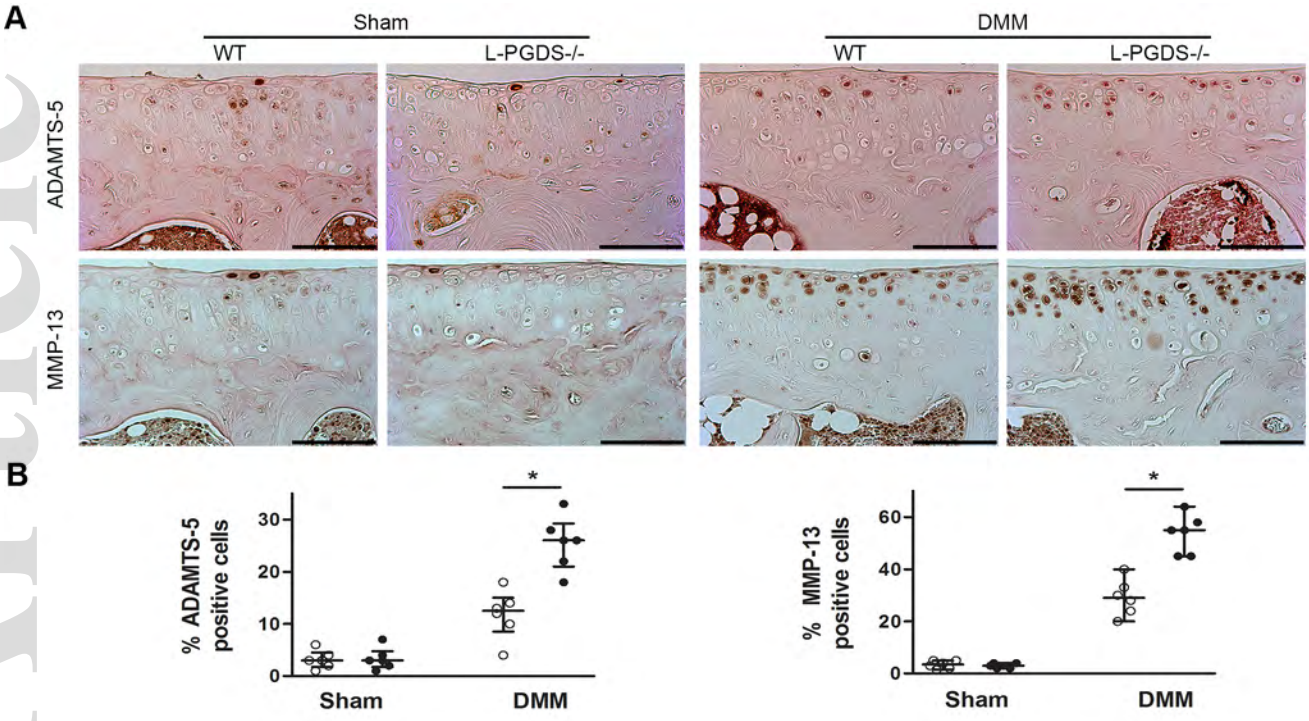

art_41297_f2.tif

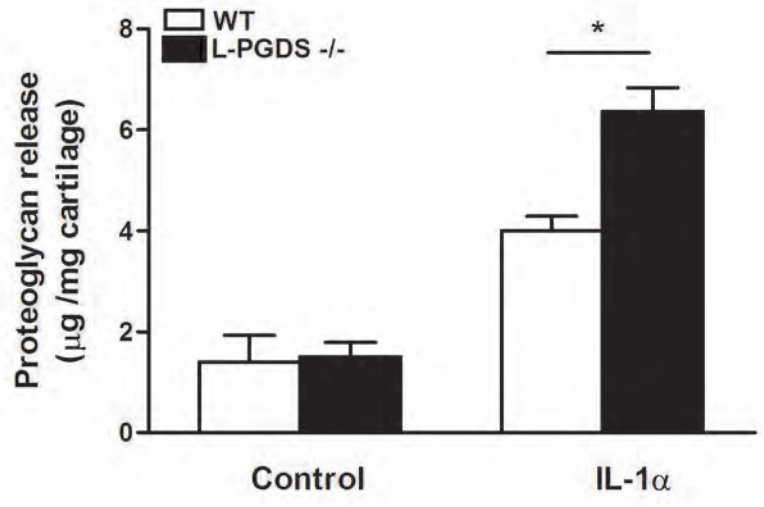

art_41297_f3.tif

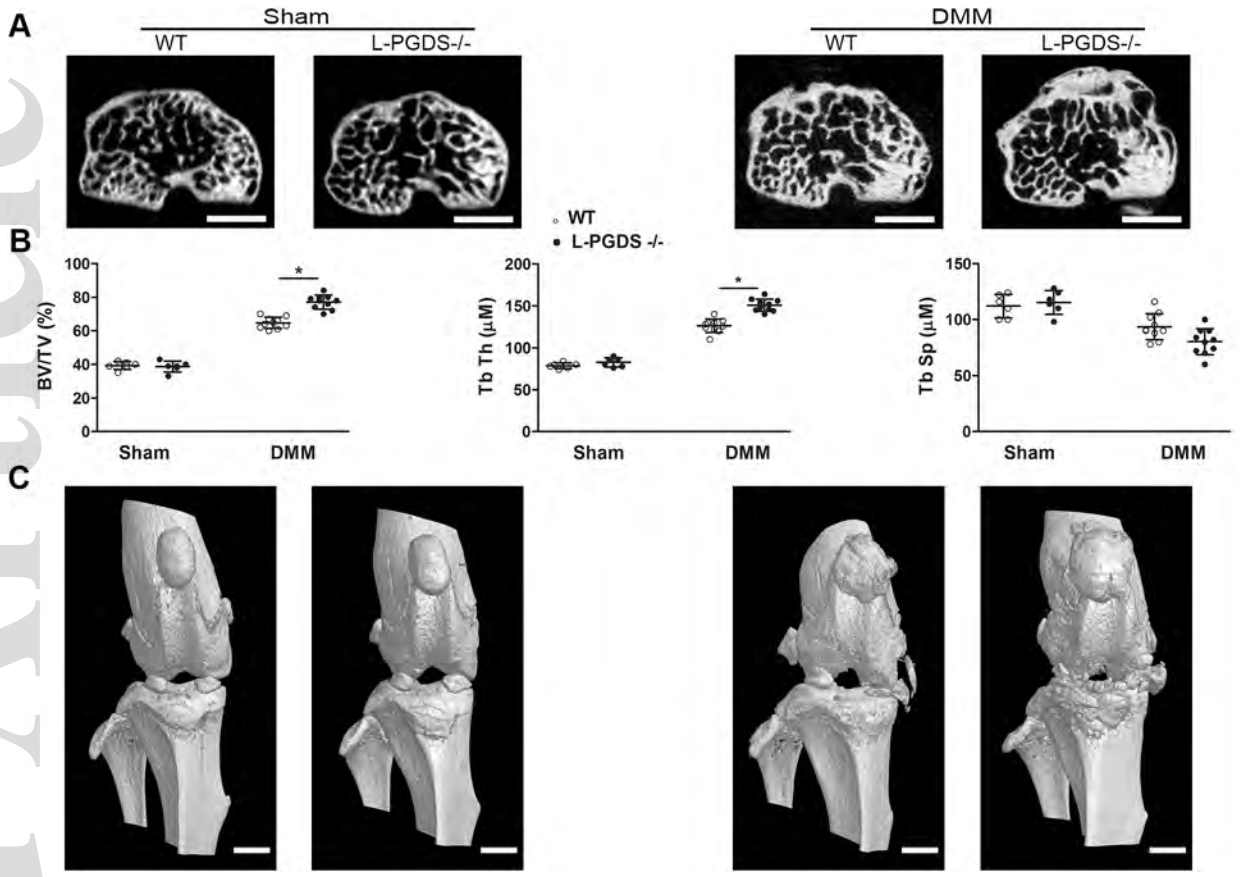

art_41297_f4.tif

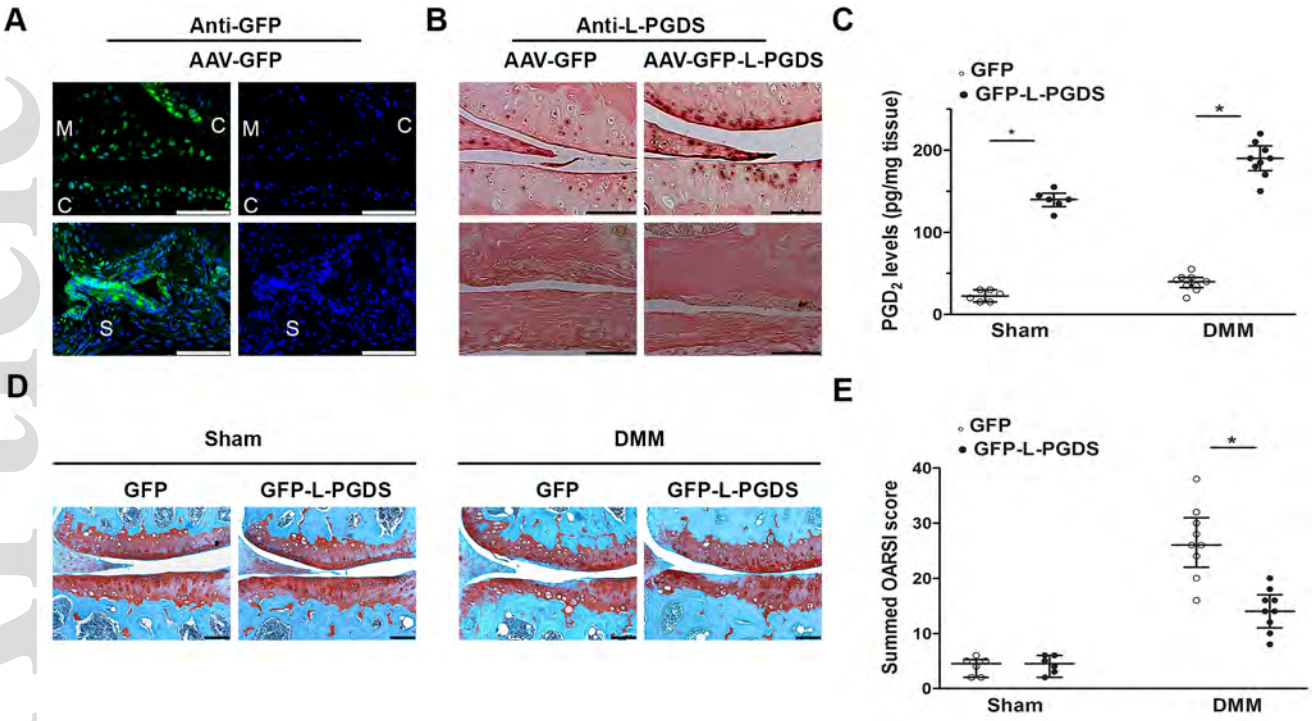

art_41297_f5.tif

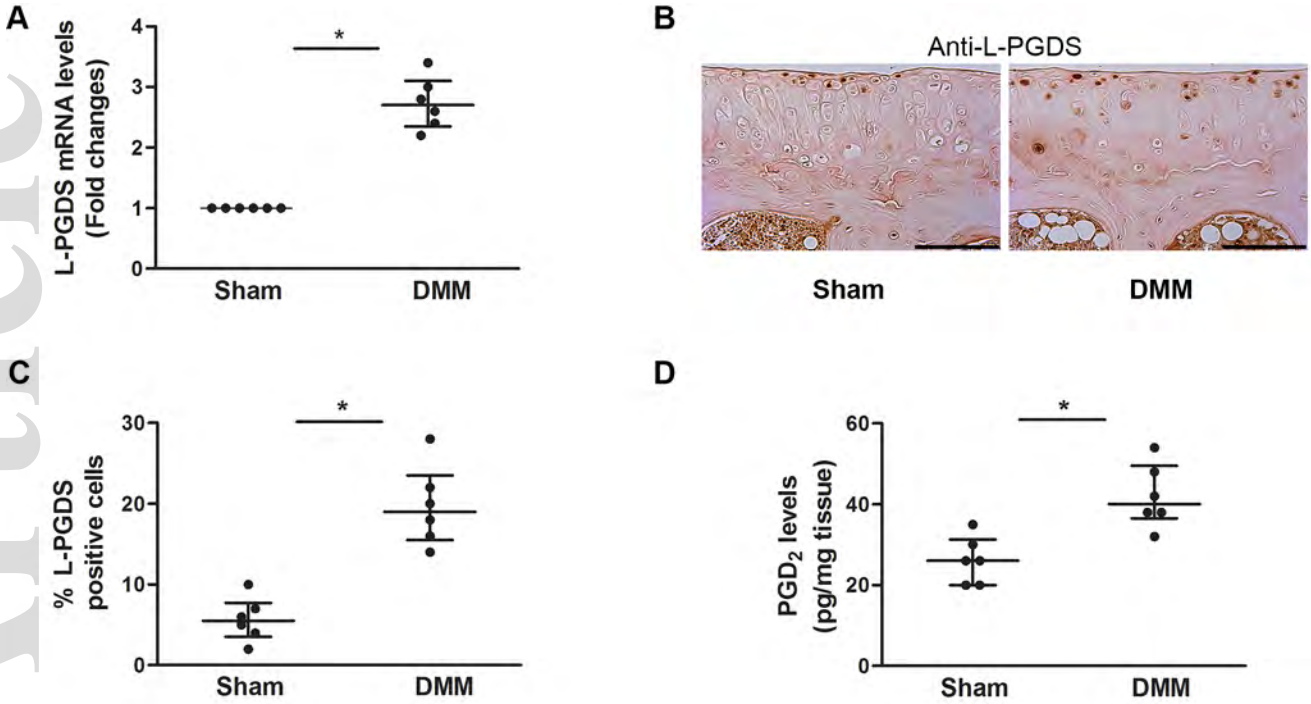

art_41297_f6.tif